2.3 Branching Dendritic Trees and Motoneuron Membrane Resistivity (1959), *Exptl. Neurol.* 1:491–527

Wilfrid Rall

This paper is concerned with both the quantitative information and the theory required for the interpretation of certain experimental results obtained with intracellular microelectrodes. The theory treats the spread of current from a neuron soma into branching dendritic trees. Formulas are derived for the calculation of membrane resistivity from physiological measurements of whole neuron resistance and anatomical measurements of soma and dendritic dimensions. The variability of available anatomical and physiological information is discussed. The numerical result is an estimated range of membrane resistivity values for mammalian motoneurons, and a corresponding set of values for the dendritic to soma conductance ratio. These values are significantly greater than those currently accepted in the literature, mainly because the dendritic dimensions appear to have been underestimated previously. Analysis of the histological evidence also reveals significant quantitative differences between infant, adult, and chromatolytic motoneurons. The theory builds upon the classical theory of axonal membrane electrotonus; all important assumptions are explicitly stated and discussed. The theory is general and can be applied to many types of neurons with many types of dendritic trees; it is also relevant to the diffusion of material in neurons. The 3/2 power of dendritic trunk diameter is shown to be a fundamental index of dendritic size. Another parameter characterizes the extensiveness of dendritic branching.

Introduction

New information about mammalian motoneurons has been obtained recently from experiments using intracellular stimulating and recording

It is a pleasure to acknowledge the stimulation provided by discussions with many colleagues; in particular, I wish to mention J. Z. Hearon, R. J. Podolsky, K. Frank, M. G. F. Fuortes, and G. L. Rasmussen. This work was begun while the author was in the Biophysics Division, Naval Medical Research Institute, National Naval Medical Center, Bethesda, Maryland; the opinions or assertions contained herein are the private ones of the writer and are not to be construed as official or reflecting the views of the Navy Department or the naval service at large.

electrodes (1, 7, 8, 12, 14). Correct interpretation of such experimental results is important because of the following implications: the electric properties of the motoneuron membrane can be estimated; the relative importance of soma and dendrites in both normal and experimental situations can be assessed; and much of accepted motoneuron physiology may require reassessment.

The interpretation of such experiments is complicated by the need to interrelate three different kinds of information: electrophysiological measurements on single motoneurons; morphological measurements of such neurons; a theory of electric current spread from a neuron soma into several branching dendritic trees. The present paper presents such a theory and applies it to the best physiological and morphological information currently available for mammalian motoneurons.

A diagrammatic illustration of the problem is provided by Fig. 1. When an intracellular microelectrode is used to apply electric current between a point inside a nerve cell body and a distant extracellular electrode (not shown in the diagram), some of the current flows directly across the soma membrane, and some of it flows into the dendrites (and axon) for varying distance before crossing the membrane. How much

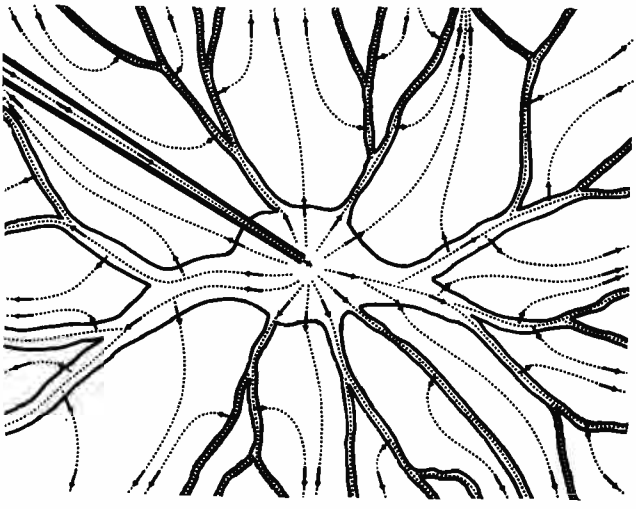

FIG. 1. Diagram illustrating the flow of electric current from a microelectrode whose tip penetrates the cell body (soma) of a neuron. The full extent of the dendrites is not shown. The external electrode to which the current flows is at a distance far beyond the limits of this diagram.

of the total current flows along each of these different paths is determined by a combination of electric and geometric factors. The electric factors, for steady state conditions, are the membrane resistivity and the specific resistivities of the intracellular and extracellular conducting media; the membrane capacity must also be considered during the transient phase of current spread. The geometric factors include the size of the neuron soma, the size and taper of all dendritic trunks, and also some measure of the amount and extent of dendritic branching.

Except for the geometric complications, this theoretical problem resembles the classical problem of passive electrotonic potential spread in axons (5, 9, 20). This fact was used in the first estimate of mammalian motoneuron membrane resistivity (8); it was assumed that the dendritic trees could be represented as cylinders of infinite length. These authors assumed six such cylinders of 5 μ diameter, for cat motoneurons; however, in their discussion (8, p. 322) they suggested that the dendritic processes must contribute rather more than their calculations had allowed. Nevertheless, this first model has become the "standard motoneurone" of Eccles (10), and a large amount of further interpretation has been based upon it. The results of the present paper indicate that this "standard motoneurone" underestimates the dendritic contribution by a significant amount.

The first interpretations of experimental transients of soma membrane potential (in response to the application of a current step across the soma membrane) were also in terms of this "standard motoneurone." Although the transient characteristics of electrotonic potential spread in long cylinders are well established for axons (9, 20), this knowledge was neglected in the estimation of the membrane time constant (6, 10, 14). The need for reinterpretation of these experiments, with suitable allowance for dendritic transient characteristics, was pointed out in preliminary communications (24, 25), and is dealt with more fully in a companion paper (26).

Theory

Assumptions

By means of the following assumptions, the geometric and passive electric properties of a neuron with dendritic trees are idealized to produce a formal theoretical model that is suitable for mathematical treatment. Definitions are introduced as needed; a complete list of all symbols is given in Appendix 1. Assumptions 1–5 are specific to the present

model; assumptions 6–8 are equivalent to assumptions already established as basic to the theory of axonal electrotonus (9, 20).

1. A dendritic tree is assumed to consist of a cylindrical trunk and cylindrical branch components. Such a tree is illustrated in Fig. 5. The analysis has been generalized to include taper, but this complication is omitted here.

2. The electric properties of the membrane are assumed to be uniform over the entire soma-dendritic surface, alternative assumptions are possible (12), but this assumption centers attention on the geometric aspects of the problem.

3. The electric potential is assumed to be constant over the entire external surface of the neuron. This is equivalent to assuming infinite conductivity of the external medium; such an assumption is commonly made for axons placed in a large volume of conducting medium. The use of this assumption can be shown to cause negligible error in the results. Briefly, this is because the gradients of electric potential to be expected in an external medium of large volume, and of reasonable conductivity, are very much smaller than the corresponding internal (axial) gradients of potential.[2]

4. The electric potential is assumed to be constant over the internal surface of the soma membrane. Together with assumption 3, this implies a uniform soma membrane potential. In this formal model, therefore, the shape of the soma surface is irrelevant, because the entire soma membrane is effectively a lumped membrane impedance. Thus lumped impedance represents the common point of origin for all dendritic trunks belonging to a single neuron. Strict validity of this assumption, during flow of current into the dendrites from an electrode placed within the soma, would imply infinite conductivity within the soma.[2]

5. The internal potential and current are assumed to be continuous at all dendritic branch points and at the soma-dendritic junction. This is an obvious physical requirement which merits explicit statement because of its importance in the mathematical treatment.

6. The electric current inside any cylindrical component is assumed to flow axially through an ohmic resistance which is inversely proportional to the area of cross section.

7. The electric current across the membrane is assumed to be normal

[2] Further assessment of assumptions 3 and 4 is presented in the discussion portion of this paper, page 521.

to the membrane surface. The uniformly distributed membrane impedance is assumed to consist of an ohmic resistance in parallel with a perfect capacity.

8. A membrane electromotive force, E, is assumed to be in series with the membrane resistance, and is assumed to be constant for all of the membrane. Under steady conditions, and in the absence of current flow, the electric potential difference, V_m, across the membrane has a resting value equal to E.

Fundamental Equations

The derivation of the differential equation for distributions of passive electrotonic potential in uniform cylinders is well established in the theory developed for axons (5, 9, 20). In regions containing no sources or sinks of externally applied current, this differential equation can be expressed

$$\lambda^2 \frac{\partial^2 V}{\partial x^2} = V + \tau \frac{\partial V}{\partial t}, \qquad [1]$$

where $V = V_m - E$ is the electrotonic potential, x represents distance along the axis of the cylinder, $\tau = R_m C_m$ is the membrane time constant, and $\lambda = [(d/4)(R_m/R_i)]^{1/2}$ is the characteristic length constant.[3]

Transient solutions of this differential equation are considered in a companion paper (26). Under steady state conditions, $\partial V/\partial t = 0$, and the general solution of the differential equation can be expressed in terms of exponential or hyperbolic[4] functions, with two arbitrary constants.

[3] A more familiar expression for λ would be $[r_m/(r_e + r_i)]^{1/2}$. Here, however, assumption 3 implies $r_e = 0$, and the resistances, r_m and r_i, for unit length, have been expressed in terms of fundamental quantities: R_m = membrane resistance for a unit area (Ωcm^2); R_i = specific resistivity of internal medium (Ωcm); and d is the diameter of the cylinder. Thus $r_m = R_m/\pi d$) and $r_i = 4R_i/(\pi d^2)$. The derivation of Eq. [1] can be indicated briefly as follows: because of assumptions 3 and 6, the axial current, I, is defined by Eq. [8], and (see Fig. 2) the membrane current per unit length of cylinder is $i_m = -\partial I/\partial x = (1/r_i)(\partial^2 V/\partial x^2)$; also, because of assumptions 3, 7, and 8, $i_m = \pi d(C_m \partial V/\partial t + V/R_m)$; equating these two expressions for i_m results in Eq. [1]. Further details can be found in Research Report NM 01 05 00.01.02 of the Naval Medical Research Institute, Bethesda, Maryland.

[4] The hyperbolic sine and cosine are tabulated functions defined as follows: $\sinh u = \frac{1}{2}(e^u - e^{-u})$ and $\cosh u = \frac{1}{2}(e^u + e^{-u})$. The properties relevant to the boundary conditions of the present problem are these: when $u = 0$, $\sinh u = 0$, and $\cosh u = 1$; also, $d/dx(\sinh u) = (\cosh u)\, du/dx$, and $d/dx(\cosh u) = (\sinh u)\, du/dx$.

The following form proves to be particularly useful for present purposes

$$V/V_1 = \cosh\,[(x_1 - x)/\lambda_0] + B_1 \sinh\,[(x_1 - x)/\lambda_0], \qquad [2]$$

where $\lambda = \lambda_0$ refers specifically to the dendritic trunk. The constant, V_1, represents the value of V at $x = x_1$, and the constant, B_1, is related to the amount of axial current flowing at $x = x_1$. For the case of a cylin-

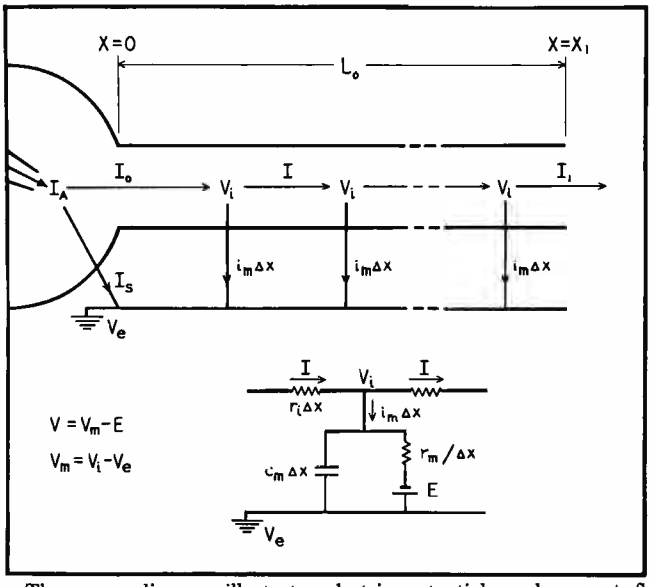

FIG. 2. The upper diagram illustrates electric potentials and current flow for a cylindrical trunk arising from a soma. The lower diagram shows the lumped parameter equivalent circuit for the membrane. Symbols are as given in the text and in Appendix 1, with the addition of Δx, which simply represents the increment in x for which quantities are lumped. The differential equations, of course, imply no lumping (i.e. the limit as $\Delta x \to 0$).

drical trunk, extending from $x = 0$ to $x = x_1$, the soma electrotonic potential, V_0, is related to V_1 by the expression

$$V_0/V_1 = \cosh\,(L_0/\lambda_0) + B_1 \sinh\,(L_0/\lambda_0), \qquad [3]$$

where $L_0 = x_1$ is the length of the trunk, see Figs. 2 and 4. The value of B_1 is determined by the branches arising at $x = x_1$, as well as by the extensiveness of subsequent branching arising from these primary branches. This dependence of B_1 upon branching is made explicit below, Eq. [16].

For the special case, $B_1 = 1$, Eq. [2] simplifies to the exponential electrotonic decrement,

$$V/V_0 = e^{-x/\lambda_0}, \qquad [4]$$

already well known for axon cylinders of infinite length. For a dendritic trunk, this solution applies only for the range $0 \leqslant x \leqslant x_1$; it implies that the branches arising at $x = x_1$ provide the same combined input conductance at $x = x_1$ as would an infinite extension of the cylindrical trunk. A value of B_1 greater than unity implies that the dendritic tree is branched more extensively than this, and a value less than unity implies less extensive branching.

Termination of a Cylinder. There are several reasons for briefly considering the special cases, $B_1 = 0$ and $B_1 = \infty$. These special cases represent particular terminal boundary conditions that are relevant, in one case, to a natural "sealed end" of a terminal dendritic branch, and relevant in the other case to experimentally produced "killed end" termination of a dendritic branch or axon. Also, these two special cases result in simplifications of Eq. [2], and they represent two extremes of electrotonic potential decrement with distance along a cylinder; these two cases are compared, in Fig. 3, with the special case, $B_1 = 1$, already considered in Eq. [4].

When $B_1 = 0$, Eq. [2] simplifies to

$$V/V_0 = \frac{\cosh\left[(x_1 - x)/\lambda_0\right]}{\cosh\left(L_0/\lambda_0\right)}, \qquad [5]$$

which is characterized by a zero slope at $x = x_1$. Curves *e*, *f*, and *g* in Fig. 3 illustrate this solution for the three lengths, $L_0/\lambda_0 = 2$, 1, and 1/2. It is clear that these curves slope less steeply than curve *a*. This solution would correspond to termination with a "sealed end" that provides a very high resistance between the internal and external media at $x = x_1$. This is a good approximation to the case of a membrane cylinder whose end is sealed with a disk composed of the same membrane; the exact solution for this case is obtained by setting

$$B_1 = \lambda_0 R_i/R_m = \left[(R_i/R_m)(d_0/4)\right]^{1/2}$$

in Eq. [2]. Thus, for example, if $R_1 = 50\ \Omega\text{cm}$, $R_m = 1250\ \Omega\text{cm}^2$, and $d_0 = 4\ \mu$, then $B_1 = 2 \times 10^{-3}$, which differs negligibly from zero.

When $B_1 = \infty$, Eq. [2] simplifies to

$$V/V_0 = \frac{\sinh\left[(x_1 - x)/\lambda_0\right]}{\sinh\left(L_0/\lambda_0\right)}, \qquad [6]$$

which is characterized by $V = 0$ at $x = x_1$. Curves *b*, *c*, and *d* in Fig. 3 illustrate this solution for the three lengths, $L_0/\lambda_0 = 2$, 1, and 1/2.

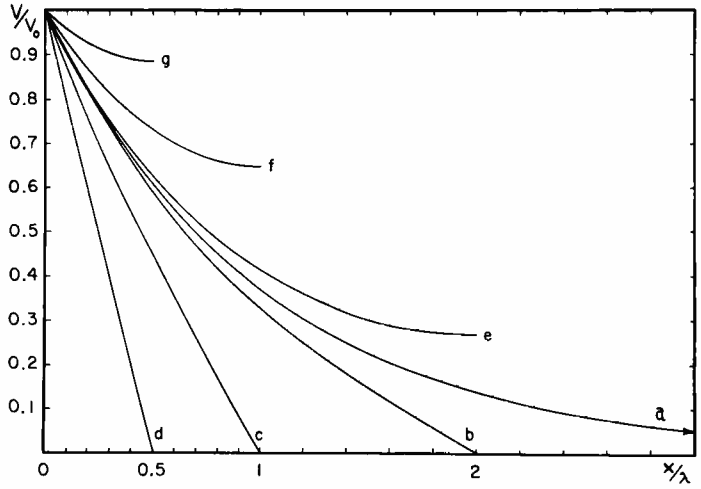

FIG. 3. Distributions of electrotonic potential along unbranched cylinders, for different terminal boundary conditions and different lengths, Eq. [2]. Curve *a* corresponds to $B_1 = 1$, or to infinite cylindrical extension, Eq. [4]. Curves *b*, *c*, and *d* correspond to $B_1 = \infty$ and $V_1 = 0$, Eq. [6]. Curves *e*, *f*, and *g* correspond to sealed end termination with $B_1 = 0$, Eq. [5].

It is clear that these curves slope more steeply than curve *a*. This solution represents part of the complete solution for a "killed end" boundary condition at $x = x_1$. When the terminal resistance between the internal and external media is essentially zero, also the terminal membrane potential difference, V_m, must be essentially zero, because the membrane EMF cannot produce an infinite current. Thus, the "killed end" boundary condition is $V = -E$ because the electrotonic potential is defined, $V = V_m - E$; in other words, this boundary condition is equivalent to application of a potential, $-E$, across an uninjured membrane at $x = x_1$. The complete solution which satisfies the two boundary conditions, $V = V_0$ at $x = 0$ and $V = -E$ at $x = x_1$, can be expressed

$$V = \frac{V_0 \sinh\left[(x_1 - x)/\lambda_0\right] - E \sinh\left(x/\lambda_0\right)}{\sinh\left(L_0/\lambda_0\right)}. \qquad [7]$$

Input Conductance of a Dendritic Tree

Because of assumptions 3 and 6, the axial current at any point, x, can be expressed

$$I = (1/r_i)\left[-\frac{\partial V}{\partial x}\right], \qquad [8]$$

where r_i represents the axial (core) resistance per unit length of the cylinder. It follows from Eqs. [2] and [8], that for the range $0 \leqslant x \leqslant x_1$,

$$I/V_1 = G_\infty \{\sinh [(x_1 - x)/\lambda_0] + B_1 \cosh [(x_1 - x)/\lambda_0]\} \qquad [9]$$

where

$$G_\infty = (\lambda_0 r_i)^{-1}$$
$$= (\pi/2)(R_m R_i)^{-1/2}(d_0)^{3/2}. \qquad [10]$$

The dendritic input current, I_0, that flows from the soma into this dendritic trunk at $x = 0$, is obtained by setting $x = 0$ in Eq. [9]. Making use of Eq. [3], the result can be expressed as the dendritic input conductance.

$$G_D = I_0/V_0 = B_0 G_\infty, \qquad [11]$$

where

$$B_0 = \frac{B_1 + \tanh (L_0/\lambda_0)}{1 + B_1 \tanh (L_0/\lambda_0)}. \qquad [12]$$

Equations [10], [11], and [12] express a very useful result. The dendritic input conductance, G_D, of any dendritic tree is expressed in terms of the reference conductance, G_∞, corresponding to an infinite extension of the cylindrical trunk, and a factor, B_0, The value of B_0 depends upon the relative trunk length, L_0/λ_0, and upon the value of B_1. The manner in which B_1 depends upon successive branchings, is considered below.

For very short dendritic trunks, B_0 essentially equals B_1, because tanh (L_0/λ_0) is then close to zero. For very long dendritic trunks, B_0 essentially equals unity, regardless of B_1, because tanh (L_0/λ_0) is then close to unity. For intermediate trunk lengths, the value of B_0 always lies between B_1 and unity.

For the special case, $B_1 = 1$, B_0 necessarily equals unity. For the limiting special case, $B_1 = 0$, which is the "sealed end" termination considered with Eq. [5], B_0 assumes its smallest possible value, tanh (L_0/λ_0).

This implies an input conductance, G_D, that is less than or equal to G_∞; it corresponds to the reduced steepness of the initial slopes of curves *e*, *f*, and *g* in Fig. 3. In the other limiting special case, $B_I = \infty$, which is related to "killed end" termination, cf. Eqs. [6] and [7], B_0 assumes its largest possible value, coth (L_0/λ_0). This implies an input conductance, G_D, that is greater than or equal to G_∞; it corresponds to the increased steepness of the initial slopes of curves *b*, *c*, and *d* in Fig. 3.

Dependence of B_1 *upon Branching*. In order to obtain an expression for B_1 in terms of subsequent branching, it is necessary to satisfy a series of boundary conditions required by assumptions 3 and 5. Continuity of both V and I at every branch point also implies continuity of the ratio, I/V, which has the dimensions of conductance.

At $x = x_1$, Eq. [9] for the dendritic trunk reduces simply to

$$I_1/V_1 = B_1 G_\infty. \qquad [13]$$

For each branch arising at $x = x_1$, there corresponds an equation similar to Eq. [9]; i.e., it is identical except for subscripts (cf. Fig. 4). For the

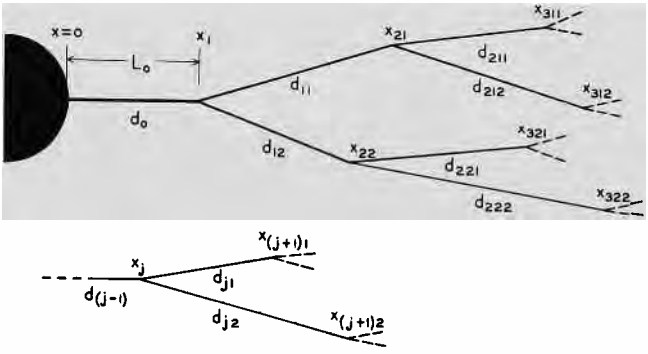

FIG. 4. Dendritic branching diagrams to illustrate the subscript notation used in the text.

*k*th branch, extending from $x = x_1$ to $x = x_{2k}$, and having a diameter, d_{1k}, a length, L_{1k}, and a characteristic length, λ_{1k}, the I/V value at $x = x_1$ can be expressed

$$I_{1k}/V_1 = B_{1k} G_\infty (d_{1k}/d_0)^{3/2}, \qquad [14]$$

where

$$B_{1k} = \frac{B_{2k} + \tanh (L_{1k}/\lambda_{1k})}{1 + B_{2k} \tanh (L_{1k}/\lambda_{1k})} \qquad [15]$$

and B_{2k} depends similarly upon branching subsequent to $x = x_{2k}$.

Continuity of I/V at $x = x_1$, requires that the sum, composed of one term like Eq. [14] for each branch arising at $x = x_1$, must equal the quantity given in Eq. [13]. This results in the expression

$$B_1 = \sum_k B_{1k}(d_{1k}/d_0)^{3/2}. \qquad [16]$$

For the common case of two unequal branches (cf. Fig. 4), this can be written

$$B_1 = B_{11}(d_{11}/d_0)^{3/2} + B_{12}(d_{12}/d_0)^{3/2} \qquad [17]$$

and for the special case of equal branches, N_1 in number, this can be written

$$B_1 = N_1(d_1/d_0)^{3/2}\left[\frac{B_2 + \tanh(L_1/\lambda_1)}{1 + B_2 \tanh(L_1/\lambda_1)}\right]. \qquad [18]$$

It can be seen that B_1 depends not only on the (primary) branches arising at $x = x_1$, but also (Eq. [15]) on the values of B_{2k}, which depend upon the (secondary) branches arising from the primary branches. This process can be repeated, step by step, until terminal branches are reached.

Generalization to any Branch Point. The results expressed in Eqs. [15] and [16] can be generalized to any branch point, $x = x_j$, of a dendritic tree (cf. Fig. 4). Thus

$$B_j = \sum_k B_{jk}[d_{jk}/d_{(j-1)}]^{3/2}, \qquad [19]$$

where

$$B_{jk} = \frac{B_{(j+1)k} + \tanh(L_{jk}/\lambda_{jk})}{1 + B_{(j+1)k}\tanh(L_{jk}/\lambda_{jk})}, \qquad [20]$$

and the subscript, jk, represents the kth branch arising at $x = x_j$; the value of λ_{jk} can be expressed

$$\lambda_{jk} = [(d_{jk}/4)(R_m/R_i)]^{1/2}. \qquad [21]$$

These general results were used to calculate Table 1.

A Hypothetical Dendritic Tree. A specific hypothetical example of an extensively branched dendritic tree is illustrated in Fig. 5. This example contains some symmetry to simplify the illustrative calculations; however, the general method does not require the presence of any symmetry. This example was also intended to be a possible approximation to some of the dendritic trees of mammalian motoneurons, on the assumption that histological preparations usually do not show the full extent of peripheral dendritic branching; how close an approximation it may be is still an open question (see pages 515 and 516).

The trunk and all branch elements are assumed to be cylinders. The trunk is assumed to have a diameter of 15 μ and a length of 50 μ. It bifurcates into two equal branches, 10 μ in diameter and 100 μ in length. All subsequent branches are assumed, for simplicity, to be 200 μ in length; their diameters, in microns, are indicated by the numbers beside

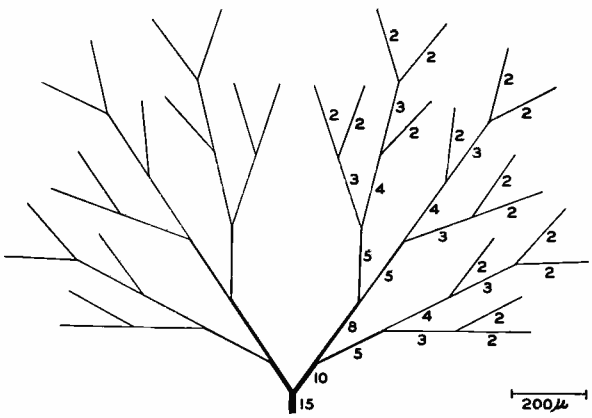

FIG. 5. Diagram of the hypothetical dendritic tree used for the calculations summarized in Table 1. The lengths and largest diameters are drawn to scale. The two halves of the tree are mirror images; the numbers represent dendritic branch diameters in microns. This two-dimensional spread is meant to represent a more compact three-dimensional tree.

them in Fig. 5. The radial extent of this system is approximately one millimeter.

To calculate the dendritic input conductance, G_D, of such a system it is necessary to assume values for the resistivities, R_m and R_i. The calculations in Table 1 have been carried out with two different values for the ratio, R_m/R_i; the larger value, 72 cm, corresponds, for example,

to $R_m = 3600\ \Omega\text{cm}^2$ and $R_i = 50\ \Omega\text{cm}$; the smaller value is one fourth of the larger. Given the R_m/R_i value, Eq. [21] is used to calculate the λ_{jk} values; then the tanh (L_{jk}/λ_{jk}) values are calculated for each cylindrical component. Beginning with $B_{(j+1)k} = 0$ for the terminal branches, the procedure is to calculate B_{jk} from Eq. [20] and then B_j from Eq. [19]. This provides the $B_{(j+1)k}$ value for a next-to-terminal branch. In this manner, step by step, the calculation approaches the dendritic trunk, where B_0 is defined by Eq. [12] and B_1 is defined by Eq. [16].

Table 1 demonstrates that, with the larger value for R_m, the extensiveness of branching is only just sufficient to make the dendritic input conductance of this tree essentially equal to the input conductance, G_∞, corresponding to an infinite extension of the cylindrical trunk. With the smaller R_m value, the same branching is more than sufficient to satisfy this criterion; in fact, the B value increases from zero to unity in only three steps; in other words, the 8-μ branches could be extended to infinity without changing the input conductance of the dendritic tree. It is clear that for smaller R_m values, less extensive branching is required to make B_0 be close to unity.

For this particular dendritic tree, the result is $G_D = 2 \times 10^{-7}$ reciprocal ohms for $R_m = 3600$ Ωcm^2, and $G_D = 4.5 \times 10^{-7}$ reciprocal ohms for $R_m = 900$ Ωcm^2. To obtain the conductance of a whole neuron, several such conductances must be added in parallel with the soma membrane conductance.

Comment. A value of B_0 greater than unity can result only when B_1 is greater than unity. If the B_{2k} values are close to unity, this depends mainly on the sum of the $(d_{1k}/d_0)^{3/2}$ values being greater than unity. The anatomical evidence does include several sets of primary dendritic branches whose diameters approximate this condition.

It is not accidental that any B_{jk} value different from unity always lies between $B_{(j+1)k}$ and unity. This is an algebraic property of Eq. [20]; it is valid for $B_{(j+1)k}$ either less than or greater than unity. Thus, whenever nature keeps the values of

$$\sum_k (d_{jk}/d_{j-1})^{3/2}$$

very close to unity, the values of B_j, as one calculates from the terminal branches to the trunk, must approach stepwise toward unity; once a value close to unity is reached, further steps cannot carry the value away from unity by any significant amount.

Whole Neuron Conductance

The whole neuron conductance, G_N, can be defined

$$G_N = I_A/V_0 = 1/R_N, \qquad [22]$$

where I_A represents the applied current flowing from an electrode within the neuron soma to an extracellular electrode, and V_0 is the steady value of the electrotonic potential at $x = 0$ (i.e., at the soma and at the origin of every dendrite), that results from this current.

TABLE 1
BRANCHING TREE CALCULATION

d_{j-1} to d_{jk}		$(d_{jk}/d_{j-1})^{3/2}$	$R_m = 3600\ \Omega\text{cm}^2$				$R_m = 900\ \Omega\text{cm}^2$			
			$\tanh (L_{jk}/\lambda_{jk})$	$B_{(j+1)k}$	B_{jk}	B_j	$\tanh (L_{jk}/\lambda_{jk})$	$B_{(j+1)k}$	B_{jk}	B_j
3 μ to	2 μ	0.54	0.32	0	0.32	0.34	0.58	0	0.58	0.62
	2 μ	0.54	0.32	0	0.32		0.58	0	0.58	
4 μ to	2 μ	0.35	0.32	0	0.32	0.47	0.58	0	0.58	0.75
	3 μ	0.65	0.26	0.34	0.55		0.50	0.62	0.85	
5 μ to	3 μ	0.46	0.26	0.34	0.55	0.70	0.50	0.62	0.85	1.02
	4 μ	0.71	0.24	0.47	0.64		0.44	0.75	0.89	
8 μ to	5 μ	0.49	0.21	0.70	0.80	0.78	0.40	1.02	1.01	0.98
	5 μ	0.49	0.21	0.70	0.80		0.40	1.02	1.01	
10 μ to	5 μ	0.35	0.21	0.70	0.80	0.88	0.40	1.02	1.01	1.05
	8 μ	0.71	0.17	0.78	0.84		0.32	0.98	0.99	
15 μ to	10 μ	0.54	0.08	0.88	0.90	0.98	0.15	1.05	1.03	1.12
	10 μ	0.54	0.08	0.88	0.90		0.15	1.05	1.03	
15 μ (at $x = 0$)			0.03	0.98	$B_0 = 0.98$		0.06	1.12	$B_0 = 1.11$	

Physical continuity of current (assumption 5) implies that the applied current, I_A, must equal the sum of the several dendritic input currents plus the current flowing across the soma membrane. Similarly, G_N is the sum of the several dendritic input conductances plus the soma conductance.

Because of assumptions 2–4, the soma conductance can be expressed

$$G_S = S/R_m, \qquad [23]$$

where S represents the soma surface area.

Making use of the results obtained for dendritic trees (Eqs. [10]–[12]), the combined dendritic input conductance can be expressed

$$\sum_j G_{Dj} = CD^{3/2}(R_m)^{-1/2} \qquad [24]$$

where

$$C = (\pi/2)(R_i)^{-1/2}, \qquad [25]$$

and

$$D^{3/2} = \sum_j B_{0j}(d_{0j})^{3/2}. \qquad [26]$$

Equation [26] defines a combined dendritic tree parameter. It shows that the combined effect of several dendritic trees is proportional, not to a simple sum or average of the trunk diameters, but to a sum composed of the 3/2 power of each trunk diameter appropriately weighted. The weighting factor, B_{0j}, relates the input conductance, G_{Dj}, of the jth trunk to its infinite cylindrical extension value, see Eqs. [10] to [12]. Because B_{0j} does depend upon R_m/R_i through $\tanh(L_{0j}/\lambda_{0j})$, the parameter, $D^{3/2}$, does not reflect purely geometric characteristics of the dendritic trees. For this reason, it is useful also to define a combined dendritic trunk parameter

$$\sum d_{0j}^{3/2} \qquad [27]$$

which does not depend in any way upon the values of R_m and R_i. It is this last parameter that is most easily estimated from histological evidence. If, in addition, study of representative dendritic trees should establish that all the B_{0j} values are close to unity, then the geometric parameter [27] would provide a good approximation to the more general parameter, $D^{3/2}$, defined by Eq. [26]. This approximation has been used in Table 2 below, but its validity is obviously subject to further testing. The following formulas are general, and are not based upon such an approximation.

Making use of Eqs. [23]–[26], the whole neuron conductance can be expressed,

$$G_N = \frac{CD^{3/2}}{\sqrt{R_m}} + \frac{S}{R_m} \qquad [28]$$

where it has been assumed that the same R_m value applies to both soma and dendrites; alternative assumptions would have to be introduced at this point.

Because the practical problem consists of estimating R_m from an experimental measurement of R_N, it is useful to solve Eq. [28] explicitly for R_m. The result is

$$R_m = (1 + \epsilon)C^2D^3R_N^2 \qquad [29]$$

where

$$1 + \epsilon = \frac{1}{4}\left[1 + \sqrt{1 + \frac{4S}{C^2D^3R_N}}\right]^2. \qquad [30]$$

When $C^2D^3R_N$ is greater than $4S$, expansion of [30] yields

$$\epsilon \approx \frac{2S}{C^2D^3R_N}.$$

For a numerical illustration relevant to mammalian motoneurons (see Table 2), consider $S = 1.25 \times 10^{-4}$ cm^2, $D^{3/2} = 2.5 \times 10^{-4}$ cm$^{3/2}$, $C = 0.2$ $(\Omega\text{cm})^{-1/2}$ and $R_N = 1.2$ megohms (7). Then $R_m = 3900$ Ωcm^2; a value of 0.083 is found for ϵ. Increase of R_N to 1.65 megohms (14) increases R_m to 7200 Ωcm^2. These values are shown in Fig. 6, which displays the theoretical relation between R_N and R_m (log-log scaling) for nine different values of the combined dendritic tree parameter, $D^{3/2}$; for this figure, it was assumed that $C = 0.2$ $(\Omega\text{cm})^{-1/2}$, which correponds to R_i between 50 and 75 Ωcm, and that $D^{3/2}/S = 2$ cm$^{-1/2}$, which corresponds to the average in Table 2.

Dendritic to Soma Conductance Ratio

The ratio of combined dendritic input conductance to the soma membrane conductance is simply the quotient of Eqs. [24] and [23]. This ratio is important in the consideration of transients (24, 26). It can be expressed

$$\rho = C[D^{3/2}/S]\sqrt{R_m}. \qquad [31]$$

Clearly, the value of ρ depends upon both geometric and electric quanti-

ties. However, when dendritic trees are such that the parameter, $D^{3/2}$, is equal to the purely geometric combined dendritic trunk parameter (compare Eq. [26] with expression [27]), then

$$D^{3/2}/S = \sum_j d_{0j}^{3/2}/S, \qquad [32]$$

and this ratio can then be regarded as purely geometric.

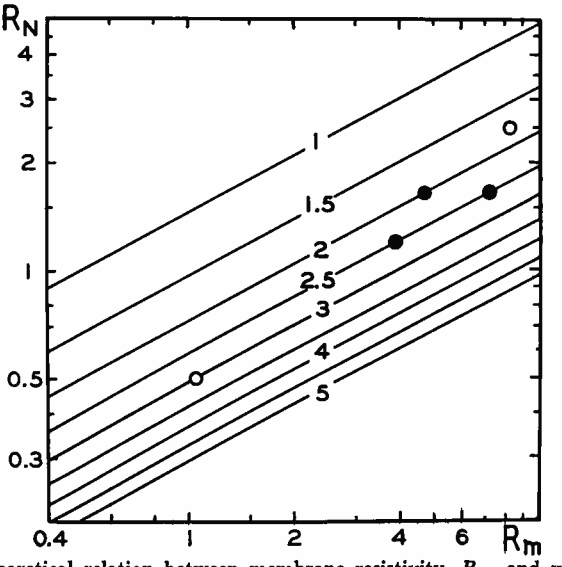

FIG. 6. Theoretical relation between membrane resistivity, R_m, and whole neuron resistance, R_N, for several values of $D^{3/2}$; note log-log scaling. R_m is in 10^3 ohm cm^2 and R_N is in megohms; the numbers in the middle represent the $D^{3/2}$ values in 10^{-4} cm$^{3/2}$. Filled circles represent specific intermediate values mentioned in the text; open circles represent extreme values of the range presented in the Results section. Because of the log-log scaling, these theoretical curves are almost, but not quite, straight lines. The calculations shared the assumptions of Eq. [33], and were based upon Eqs. [28] and [34].

For the motoneurons of Table 2, this geometric ratio has an average value of about 2 cm$^{-1/2}$; using also $C = 0.2$ $(\Omega\text{cm})^{-1/2}$, Eq. [31] yields the particular numerical formula

$$\rho = 0.4\sqrt{R_m} \qquad [33]$$

where R_m must be expressed in Ωcm^2. This implies, for example, that values of 400, 1600, 3600, and 6400 Ωcm^2 for R_m, would correspond to values of 8, 16, 24, and 36 for the ratio, ρ.

For the interpretation of experimental evidence, it should be emphasized that ρ depends upon R_m as well as upon geometry, and that the determination of R_m from the data cannot depend upon the value of ρ (unless a trial and error procedure is employed). The direct procedure for calculation of R_m makes use of Eq. [29]. However, in calculations where a value of R_m is assumed (e.g., Table 2), it is efficient to calculate ρ from Eq. [31], or from formula [33] when applicable, and then to calculate R_N from the relation

$$R_N = \frac{R_m}{(\rho + 1)S} \qquad [34]$$

which follows from the definitions (or from Eqs. [28] and [31]).

Anatomical Information

Ideally, for present purposes, the soma and dendritic dimensions should be those of the same neuron upon which the electrophysiological measurements have been made, and the dimensions should be those of the living neuron. Instead, it is necessary, at present, to use the morphological dimensions of one sample of dead cells in combination with physiological results obtained from a different sample of living, but not completely normal cells. Because of uncertainty in how well these two samples are matched, there is also uncertainty in the interpretations. It is therefore important to consider the variability of the data and the possibilities for systematic error.

The information summarized in Table 2 was obtained by measurement of published histological material, which is identified in the footnotes. These neurons were all large ventral horn cells from the lumbar region of mammalian spinal cord. Although the motor axon was not identifiable in every case, it is generally assumed that such cells are the same as the motoneurons which neurophysiologists have been studying with intracellular microelectrodes.

This quantitative sample is small and is based upon histological illustrations that were not specifically intended for such measurements. I hope that this study will stimulate neurohistologists to provide more extensive measurements from the best possible original material.

Other Anatomical Sources. Ramón y Cajal presented a wealth of material relevant to the present study. There are, however, two disadvantages: Most of his illustrations are from fetal material, and the scale is not given in his figure legends. For the present study, such

illustrations as his Figs. 129–131 (27) are especially interesting for the extensiveness of branching that they reveal.

Balthasar (2) has presented a histological study of normal and chromatolytic motoneurons in young cats (ages up to 6 months). Although this study contains considerable information on the dendrites, the published figures are of limited value for present purposes, because the sections were 12 to 20 μ in thickness, and no reconstruction from serial sections was presented. In any single section, some dendritic trunks are likely to be missed completely, and even those which do appear may not display their full diameters. However, even with these disadvantages, measurements of Balthasar's figures reveal general agreement with the results presented in Table 2. Balthasar has been cited by Eccles in support of his "standard motoneurone" (10, p. 6; 7, p. 514). In fact, Balthasar emphasizes the differences between several types of cells with different dendritic complement (2, pp. 356–358, 362–364, 377). Balthasar reports that dorsolateral tibial neurons have 5 to 10 finer dendritic trunks, of which 1 or 2 are thicker (principal dendrites); central tibial neurons usually have about 4 to 7 dendritic trunks of relatively larger caliber; peroneal neurons usually have 3 to 5 relatively even thicker trunks. He does not give values for these various trunk diameters, but measurements of his figures (in photographic enlargement) give diameters of about 19 μ for the larger dendritic trunks of peroneal neurons (presumably not chromatolytic in his Figs. 7a, b), and diameters from 12 to 20 μ for the principal dendrites of chromatolytic tibial neurons (his Figs. 3a and 7a, b). The smallest dendritic trunks of the chromatolytic tibial neurons appear to be around 4 to 7 μ in diameter. With such diameters, the three neuron types (cited above) all seem to imply values between 200 and 300 $\mu^{3/2}$ for the combined dendritic trunk parameter, in agreement with the results in Table 2.

Systematic Error. A serious possibility of systematic error is the possibility of swelling and/or shrinkage that may take place during various stages of death and fixation. There is evidence, for example, which indicates dendritic swelling in the cerebral cortex under conditions of anoxia (29); the possibility of such an effect in the spinal cord remains to be determined. On the other hand, histologists often estimate fixation shrinkage as much as 15 per cent (in linear dimensions) or more. There is the possibility of unknown osmotic shrinkage or swelling in Chu's preparations (4). With regard to peripheral branching, experienced anatomists appear to agree that the true branching must be more exten-

TABLE 2

MAMMALIAN MOTONEURONS

Mammal	Geometric quantities: Dendrites $\Sigma d^{3/2}$[a] (10^{-6} cm$^{3/2}$)	Geometric quantities: Soma S[b] (10^{-6} cm^2)	Geometric quantities: Ratio $\Sigma d^{3/2}/S$ (cm$^{-1/2}$)	Hypothetical estimates[h] (for $R_m = 4000$ Ωcm^2): ρ	(for $R_m = 4000$ Ωcm^2): R_N (megohms)	(for $R_m = 600$ Ωcm^2): ρ	(for $R_m = 600$ Ωcm^2): R_N (megohms)
Human, adult							
(Chu)[c]							
Fig. 2	249	149	1.67	21	1.21	8.2	0.44
Fig. 3	205	129	1.59	20	1.47	7.8	0.53
Fig. 12	281	103	2.73	34	1.09	13.4	0.40
Fig. 13	226	109	2.07	26	1.35	10.1	0.50
Fig. 18	217	87	2.49	32	1.41	12.2	0.52
Fig. 21	244	98	2.49	32	1.26	12.2	0.46
Mean	237	112	2.17	27	1.30	10.6	0.48
Standard Deviation	27.1	22.7	0.47	5.9	0.14	0.23	0.05
Cat, adult							
(Haggar and Barr)[d]	204	94	2.17	28	1.49	11	0.55
(corrected for shrinkage)	261	130	2.01	25	1.17	10	0.43
(Fatt)[e]	226	107	2.11	27	1.35	10	0.50
Cat, "Standard Motoneurone"							
(Eccles, 1957)[f]	67	150	0.45	5.7	4.0	2.2	1.25
(Coombs, *et al.*, 1959)[f]	78	150	0.52	6.6	3.5	2.6	1.13
Human, adult, chromatolytic							
(Chu)[c]							
Fig. 14	80	73	1.1	14	3.7	5.4	1.28
Fig. 15	104	126	0.83	10	2.8	4.1	0.93
Mean	92	100	0.92	12	3.2	4.5	1.09

TABLE 2 (*Continued*)

Mammal	Geometric quantities: Dendrites $\Sigma d^{3/2}$[a] (10^{-6} cm$^{3/2}$)	Geometric quantities: Soma S[b] (10^{-6} cm^2)	Geometric quantities: Ratio $\Sigma d^{3/2}/S$ (cm$^{-1/2}$)	Hypothetical estimates[h] (for $R_m = 4000$ Ωcm^2): ρ	(for $R_m = 4000$ Ωcm^2): R_N (megohms)	(for $R_m = 600$ Ωcm^2): ρ	(for $R_m = 600$ Ωcm^2): R_N (megohms)
Human, infant (Chu)[c]							
Fig. 1	100	63	1.59	20	3.0	7.8	1.08
Fig. 5	113	49	2.31	29	2.7	11.3	1.0
Fig. 6	135	76	1.78	22	2.2	8.7	0.81
Fig. 7	132	75	1.76	22	2.3	8.6	0.83
Fig. 20[g]	83	29	2.87	36	3.7	14.1	1.37
	(139)	(58)	(2.40)	(30)	(2.2)	(11.8)	(0.81)
Mean[g]	113	58	2.06	26	2.7	10.1	0.93
	(124)	(64)	(1.97)	(25)	(2.4)	(9.7)	(0.88)
Standard Deviation[g]	21.9	19.8	0.53				
	(16.6)	(11.3)	(0.36)				

[a] Combined dendritic trunk parameter, see Eq. [26] and [27]. The dendritic trunk diameters were measured at distances about 20 to 40 μ beyond their points of origin from the soma. This avoids most of the ambiguity due to sharp taper at dendritic origins. In many cases, the dendritic trunk is almost cylindrical from this point of measurement to the region where branching occurs; some swelling is often seen just before a branch point. These diameter values are subject to a measurement error of about 10 per cent; the possibility of systematic error is considered elsewhere.

[b] Estimate of soma surface area. The measurement consisted of estimating a major and a minor diameter (approximately perpendicular to each other). An attempt was made to exercise good judgment in adjusting the major diameter to include some allowance for proximal dendritic portions of particularly large diameter. The soma surface, S, was then estimated as π times the product of the major diameter and the minor diameter; this is an approximation to the surface area of an ellipsoid. Such estimates of soma surface area may well be subject to 25 per cent error or more, and it is not clear how they can be much improved upon without three-dimensional information. There is, of course, some arbitrariness in distinguishing between soma and proximal dendrites, because there is actually a transition from the large internal cross section of the soma, to the small internal cross section of a dendritic trunk.

TABLE 2 (*Continued*)

[c] Chu (4) presented photographs of human anterior horn cells isolated from fresh autopsy material. Although it is probable that the method of cell isolation resulted in breakage of peripheral dendritic branches, the dendritic trunks are probably all present. The origins of a few trunks may be hidden behind the soma, but most of them can be measured from the photographs. The number of dendritic trunks ranges from from 7 to 12; the apparent diameters range from about 2.5 to 10 μ for infants, and from about 4 to 15 μ for adults; there are a few 20-μ diameter trunks which bifurcate into smaller trunks after a short distance. Although these cells were not subject to fixation shrinkage, there remains a possibility of osmotic shrinkage or swelling; no attempt is made here to estimate this. Two sets of measurements were made several months apart; a comparison of these indicates reproducibility within about 10 per cent error.

[d] Haggar and Barr (18) presented in their Fig. 3, a photograph of a model of an adult cat motoneuron. This model represents a reconstruction from serial sections of 4-μ thickness. Thus, all of the dendritic trunks, regardless of their orientation relative to the plane of sectioning, have been included. Reasonably satisfactory measurements can be made from the photograph; however, a personal communication from Professor Barr provides the following approximate measurements from the actual model: the two large dendrites have diameters of about 16 and 19 μ; there are six small dendrites with an average diameter of about 4.5 μ; the mean diameter of the soma is about 50 μ. In estimating the soma surface area, I used a major diameter of 60 μ and a minor diameter of 50 μ. Professor Barr estimated the shrinkage produced by their histological methods as about 10 to 15 per cent, in terms of linear dimensions; the larger figure implies a correction factor of $(0.85)^{-3/2} = 1.28$ for the combined dendritic trunk parameter, and a factor of 1.38 for the soma surface area. Professor Barr also pointed out that the purpose of the model was illustrative rather than high precision. In view of the 200 × magnification used in the model, it seems reasonable to me to hope that the resulting measurements are subject to not more than about 10 per cent error.

[e] Fatt (11) presented in his Fig. 1, a camera lucida drawing of a large Golgi-stained neuron (presumably a motoneuron) in the ventral horn of an adult cat's spinal cord. Because the section was 0.25 mm thick, this should display all of the dendritic trunks, except those whose projections are hidden by the soma itself. Although Fatt makes no claim for high precision in the dendritic diameters of his camera lucida drawing, a photographic enlargement of his published figure was measured with the following results: the dendritic diameters in microns are about 14.2, 12.3, 11.3, plus two of 9.4 and two of 6.6; the soma major and minor diameters are about 95 and 40 μ. It is possible that these values should be increased to correct for shrinkage; it is also possible that 1 or 2 dendritic trunks are hidden by the soma. No correction has been made for these possibilities; consequently, the values given in the table are believed to be conservative (i.e., low rather than high).

[f] The "standard motoneurone" of Eccles (10) was based upon the illustrative example introduced by Cooms, Eccles, and Fatt (8). This consisted of a spherical soma, 70 μ in diameter, and six dendrites of 5 μ diameter and infinite length. A

TABLE 2 (*Continued*)

later version (7) added one more 5-μ diameter cylinder to take the axon into account. Both versions of this "standard motoneurone" are included for comparison with the measurements.

[g] Two sets of values are given for Chu's Fig. 20. The first set of values corresponds to the magnification (340) given in his figure legend. Because comparison of Fig. 20 with Figs. 5 and 21 suggests that this magnification might be incorrect, a second set of values (enclosed by parentheses) was calculated for magnification (240), which is the same as that for the adjacent Fig. 21.

[h] The dendritic to soma conductance ratio, ρ, is defined by Eq. [31], and the whole neuron resistance, R_N was calculated from Eq. [34]. It was assumed that the combined dendritic tree parameter, Eq. [26], could be approximated by the combined dendritic trunk parameter, expression [27]. This assumption is subject to modification as more complete information becomes available; it is based upon the theoretical considerations discussed in connection with Fig. 5 and Table 1, and upon a few branching measurements cited in this paper, below. It was also assumed that $C = 0.2$ $(\Omega\text{cm})^{-1/2}$, which corresponds to R_i between 50 and 75 Ωcm; this provides no significant source of uncertainty. The 600 Ωcm^2 value for R_m corresponds to the latest estimate of Eccles and his collaborators (7), while the 4000 Ωcm^2 value was chosen to bring the calculated adult mean of Table 2 into approximate agreement with the mean R_N value obtained experimentally.

sive than that usually seen in histological preparations.[5] The difficulties include incompleteness of staining, loss into neighboring histological sections, and (in the case of Chu's preparations) loss by fragmentation.

It would be very unrealistic to assume that Table 2 is free of systematic errors. These values simply represent an attempt at a current best estimate, based on recent published evidence.

Comparison of Geometric Quantities

Several significant differences and similarities between the various neurons are suggested by inspection of Table 2. These have been tested for statistical significance by means of the "t" test (13), which is appropriate for such small samples on the usual assumption of unbiased sampling from an underlying normal distribution.

The two adult cat neurons are in good agreement with the sample of six adult human neurons. With respect to the values listed in Table 2, they may be treated as a combined sample from a single population. The t statistic, with 5 degrees of freedom, gives probabilities in the range 0.3 to 0.7 for such deviations.

Comparison of the six adult human cells with the five infant human cells reveals that the infant cells are significantly smaller. The average infant values for both $\Sigma d^{3/2}$ and S are about one half the average adult values. Values of the t statistic obtained for the difference between infant and adult means give a probability less than 0.001 for the $\Sigma d^{3/2}$ values, and a probability less than 0.01 for the S values, that these two samples would be obtained by chance from a single population. The good agreement between infant and adult mean values of the ratio, $\Sigma d^{3/2}/S$, indicates that $\Sigma d^{3/2}$ and S are comparable indices of neuron size. It also indicates a tendency to preserve this ratio and the related ratio, ρ, during growth.

Comparison of the two human chromatolytic cells with the six human adult cells reveals, contrary to the usual statements about degenerative swelling, that the abnormal dendrites are significantly smaller, and that the abnormal soma is also smaller, but not significantly so. In the case of the dendrites, the t statistic gives a probability less than 0.01 that such a deviation could have occurred by chance. This was an unexpected result in view of the usual references to degenerative swelling; Chu's

[5] It is a pleasure to acknowledge helpful discussions of this and related questions with Dr. Grant L. Rasmussen.

figure legends refer to a "swollen cell-body." In these two cases, at least, the swelling is an optical illusion due to dendritic shrinkage. These two cells may not correspond to the more acutely degenerate cells that have been studied electrophysiologically.

The "standard motoneurone" of Eccles (7, 10) is significantly different from both the adult and infant neurons in Table 2. It does not satisfy the usual statistical criteria for being a probable mean from these cell populations. Comparison of the $\Sigma d^{3/2}$ value (for either "standard motoneurone") with the group of eight adult neurons gives a value of the t statistic, which implies a probability less than 0.001 for chance occurrence of such a deviation. The "standard motoneurone" value for the ratio, $\Sigma d^{3/2}/S$, is about one-fourth the mean value found for both adult and infant neurons; the t statistic gives a probability of less than 0.01 for chance occurrence of such a deviation. The "standard motoneurone" may not be significantly different from the two chromatolytic cells.

Dendritic Diameter Change with Branching

It is important to know how the value of $\Sigma d^{3/2}$ changes as one considers successive branchings in a dendritic tree. The value of B_0 for any given dendritic tree depends most strongly upon the first few branchings (i.e., of the trunk and major branches); this can be seen by considering the branching calculations summarized in Table 1, accompanying Fig. 5.

Obviously, careful measurements ought to be made with the most suitable obtainable histological preparations. A few tentative results are given here based upon some of the published histological illustrations already referred to. The examples shown here include only the first one or two branchings. They indicate that the value of $\Sigma d^{3/2}$ increases somewhat with branching. When measurements are extended to more peripheral branching, it is important to guard against spuriously low values; these could result from loss of branches due to thin sections, incomplete staining, or fragmentation.

Haggar and Barr's photograph (18) provides a little information about branching. The 16-μ trunk gives off two branches, 4.5 and 5 μ, while becoming itself reduced to 13 μ in diameter; thus the trunk $d^{3/2}$ value of 64 $\mu^{3/2}$ is exceeded by a larger $\Sigma d^{3/2}$ value of 67.7 $\mu^{3/2}$. There is also a 6.5-μ trunk which bifurcates into a 5- and a 4-μ branch; here the trunk $d^{3/2}$ value of 16.6 $\mu^{3/2}$ is exceeded by a larger $\Sigma d^{3/2}$ value of 19.2 $\mu^{3/2}$.

Chu's Fig. 3 (4) has a trunk at 6 o'clock which is about 10 μ in

diameter and gives rise to two branches about 7.5 and 6 μ; farther out, these have become three branches about 6, 5, and 4.5 μ. The $\Sigma d^{3/2}$ value goes from about 31.5 $\mu^{3/2}$ for the trunk, to about 35 $\mu^{3/2}$ for the two and also the three branches. This cell also has a 9-μ trunk at 10 o'clock which gives rise to two branches about 7.5 to 5 μ, and then three branches about 5, 5, and 3.5 μ. The $\Sigma d^{3/2}$ values go from about 27 $\mu^{3/2}$ to about 32 $\mu^{3/2}$, and then to about 29 $\mu^{3/2}$.

Clearly, better and more extensive measurements are desirable. These measurements do suggest, when considered together with Fig. 5 and Table 1, that motoneuron dendritic branching may exceed the amount necessary to make $B_0 = 1$ and may thus make the combined denditric tree parameter greater than the combined dendritic trunk parameter. If this should prove to be the rule, then R_N values calculated for any given R_m (Table 2) will become smaller; conversely, larger R_m values will be implied by any given experimental R_N value.

Histological Questions

These preliminary results raise a number of questions requiring further study. Among these are the following: How extensive is the peripheral branching of mammalian motoneuron dendrites? Will further study confirm that the value of $\Sigma d^{3/2}$ increases when calculated for successive branchings of a dendritic tree? For how many branchings can this be reliably tested? Can the shrinkage and/or swelling of dendrites resulting from death and fixation be reliably estimated? Can satisfactory methods be devised for histological measurement of the same cell upon which physiological measurements have been made? Will further study confirm that acute chromatolytic somas only appear to be swollen because of shrunken dendrites? Are there important geometric differences between acute and chronic chromatolytic cells? Will further study confirm the proportionality found (on the average) between soma surface area and the combined dendritic trunk parameter, during growth from infant to adult? Do similar relations hold for other types of neurons?

Results with Comments

The purpose here is to compare the anatomical information of Table 2 with electrophysiological measurements of whole neuron resistance, R_N, obtained with cat motoneurons. This leads to an estimated range of R_m values within which the unknown R_m value of mammalian motoneuron membrane is most likely to lie.

Physiological-Anatomical Matching

Electrophysiological R_N *Values.* Frank and Fuortes (14) reported a mean value of 1.65 megohms for fifty-two cat motoneurons; the eleven values listed in column 8 of their Table I have a mean of 1.5 megohms, and a statistical variance whose best estimate is 0.32 (megohms)^2, implying a standard deviation of 0.57 megohm. More recent results,[6] obtained with larger tipped micropipettes, give a lower mean value of about 1.2 megohms.

The earlier measurements of Coombs, Eccles, and Fatt (8) have been extended by the results recently reported for twenty-five cat motoneurons by Coombs, Curtis, and Eccles (7). These twenty-five values have a mean of 1.14 megohms, and a statistical variance whose best estimate is 0.22 (megohms)^2, implying a standard deviation of 0.47 megohm.

Both sets of measurements lie in the range from 0.5 to 2.5 megohms. The ratio between the two variances is not statistically significant (13). When the eleven tabulated values of Frank and Fuortes (14) are compared with the twenty-five values of Coombs, Curtis, and Eccles (7), the t test gives a probability slightly greater than 0.05 that this much difference between means would occur by chance (13), if sampling were from a single normal population; i.e., the difference is probably not significant. The combined sample of thirty-six motoneurons has a mean of 1.25 megohms, and a variance whose best estimate is 0.27 (megohms)^2, implying a standard deviation of 0.52 megohm.

Comparison with Table 2. For $R_m = 4000\ \Omega\text{cm}^2$, the mean of the calculated R_N values for adult motoneurons in Table 2 agrees quite well with the above-mentioned physiological measurements. However, the variance of the calculated R_N values has a best estimate of 0.019 (megohms)^2, for the six adult human cells. This is smaller than the physiological variance by a factor of about 14. This variance ratio has a probability less than 0.01 of occurring by chance (13), if sampling were from a single normal population; i.e., this ratio is probably significant.

Variance Discrepancy. The problem is to find a satisfactory explanation for the fact that the spread of physiological values corresponds to nearly four times the spread in anatomical size. The most important variability in anatomical size is that of the combined dendritic parameter,

[6] Personal communication from Drs. Frank and Fuortes.

as may be seen from the large values found for the dendritic to soma conductance ratio, ρ, in Table 2. It is therefore relevant to note the possible importance of variability between motoneurons with respect to the extensiveness of their branching. This could produce a variability in the combined dendritic tree parameter that would be greater than that of the combined dendritic trunk parameter. This possibility, as well as the possibility of unknown selection in this small anatomical sample, can be checked by further histological study.

Another possibility is that there could be variability in R_m superimposed upon size variability. Unless direct evidence is obtained for this, I prefer the hypothesis that these cat motoneurons are closely similar in their passive membrane resistivity.

It is possible that the larger physiological variance is partly due to variability in experimental recording conditions and in physiological trauma. Such variability is difficult to assess. For example, it is known that small neurons are more liable to serious injury upon penetration by a micropipette than are the larger neurons. This would be expected to bias the physiological sample toward the larger cells in a given population; the largest R_N values would tend to be lost and low R_N values would predominate. Evidence in support of this is provided by the observation[7] that average R_N values fell when the tip size of the micropipette was increased. This effect would lower both the mean and the variance of R_N. The effect of injury upon cells included in the physiological sample would also be in the direction of low R_N values; this would also tend to lower the mean value obtained for R_N, but it would probably increase the variance. Occasionally, clogging of a micropipette tip can produce a high resistance value, but this effect is probably secondary to those already mentioned.[7] The net result of all these factors upon the variance of R_N is not clear. It may be expected that the mean value obtained for R_N will be lower than the "correct" value, but the magnitude of this discrepancy is not known.

Membrane Resistivity

Because of the uncertainties considered above, the membrane resistivity of cat motoneurons is probably best estimated in terms of a range of

[7] Personal communication from Drs. Frank and Fuortes. It is a pleasure to acknowledge helpful discussions of this and related questions with Drs. Frank and Fuortes.

values. On the basis of the evidence considered here, this range extends approximately from 1000 to 8000 Ωcm^2.

The low end of this range corresponds to the possibility that the lowest R_N values, around 0.5 megohm, actually represent the true resistance values of large cells with $D^{3/2}$ values around 300 $\mu^{3/2}$. The high end of this range corresponds to the possibility that the largest R_N values, around 2.5 megohms, actually represent the true resistance values of small cells with $D^{3/2}$ values around 180 $\mu^{3/2}$; see Fig. 6.

However, if the mid-range of the physiological samples corresponds with the mid-range of the anatomical sample, a value around 4000 to 5000 Ωcm^2 would be indicated for R_m. Then the R_N value of 1.2 megohms (7) would correspond to a $D^{3/2}$ value of about 250 $\mu^{3/2}$. The 1.65-megohm value of Frank and Fuortes (14) was obtained with finer microelectrodes and may have been less weighted for the largest motoneurons; thus, while a 250-$\mu^{3/2}$ value for $D^{3/2}$ would imply $R_m = 7000$ Ωcm^2 for this R_N value, a reduction of $D^{3/2}$ to 200 $\mu^{3/2}$ would imply $R_m =$ 4700 Ωcm^2.

Such values for R_m are larger than the values of 500 (8), 400 (10), and 600 (7) Ωcm^2 proposed by Eccles and his collaborators. Most of this difference can be attributed to a difference in estimation of dendritic dimensions; see "standard motoneurone" in Table 2. This difference is surprising because essentially the same anatomical sources (2, 4, 18) were cited by Eccles (10, pp. 2–6) as the basis for his "standard motoneurone." The statistical improbability of this "standard motoneurone" is assessed on page 515 of this paper. All of these estimates share whatever systematic error may be present.

Dendritic to Soma Conductance Ratio

A range of probable values for this conductance ratio can be obtained by combining the R_m values, considered above, with the values found for the purely geometric ratio in Table 2. The geometric size ratio, Eq. [32], has a mean value of about 2.1 $cm^{-1/2}$, with a standard deviation of about 0.4, for the combined population of eight adult plus 5 infant mammalian neurons in Table 2. There seems to be no significant correlation between neuron size and the value of this ratio. Therefore, the most probable values of the conductance ratio, ρ, can be expected to lie in a range, plus or minus one standard deviation, for any particular value of R_m. Using Eq. [31], with $C = 0.2$ $(\Omega cm)^{-1/2}$, the following ranges of probable ρ values are obtained: at one extreme, with $R_m = 1000$ Ωcm^2, this range

extends approximately from 10 to 16; at the other extreme, with $R_m = 8000\ \Omega cm^2$, this range extends approximately from 31 to 47; for the mid-range of 4000 to 5000 Ωcm^2, this probable range of ρ values extends approximately from 21 to 35.

All of these values are significantly larger than the value of 2.3 used by Eccles and his collaborators (7, 8, 10); see especially (7, p. 518). This discrepancy merits explicit mention, because of the interpretations which have been based upon the 2.3 value; it may be attributed to the difference between the "standard motoneurone" and the measurements summarized in Table 2; these differences have already been commented upon above. The factor of about 10 between this 2.3 value and the mid-range, 21 to 35, cited above, can be seen (in Table 2) to be composed of two factors: a factor of about 4 in the geometric ratio, $\Sigma d^{3/2}/S$, and a factor of about 2.5 in the value of $\sqrt{R_m}$.

Large values of ρ provide a measure of the dominance of dendritic properties over somatic properties in determining various whole neuron properties of motoneurons. Clearly, the conductance is predominantly dendritic. The above values further strengthen the case (24, 26) for dendritic dominance in the passive transient response of the motoneuron membrane to a current step applied at the soma. The case for dendritic dominance in the modulation of a facilitatory synaptic potential also depends upon large ρ values; this leads naturally to a possible functional distinction between dendritic and somatic synaptic excitation: the larger and slower dendritic contribution would be well suited for fine adjustment of central excitatory states, while the relatively small number of somatic synaptic knobs would be well suited for rapid triggering of reflex discharge. Such implications will be developed further in a subsequent paper.

Discussion

Generality of the Theory

The theory and the resulting method of analysis are clearly more general than the particular applications presented as Results. The applicability of the theory to motoneurons is not contingent upon the correctness of the particular anatomical and physiological estimates presented here; the possibility of systematic error has been pointed out; as better data become available, these can be fed into the general theoretical results. The same method of analysis is also applicable to other types of neurons. Of particular interest are the dendritic trees of Purkinje cells

and of pyramidal cells, both of which have been subjected to recent quantitative study.

Diffusion Analogy. All of the theoretical results obtained in this paper are also applicable to the diffusion of material (without convection) from a steady source within the soma to a constant low extracellular concentration, or to diffusion from a constant high extracellular concentration to a steady sink within the soma. In this context, the intracellular source could represent either metabolic production of a substance within the soma, or active inward transport across the soma membrane; similarly, the intracellular sink could represent either metabolic consumption of a substance within the soma, or active outward transport across the soma membrane. Free diffusion along the dendritic core and across the soma and dendritic membrane would be assumed.

For example, Eq. [31] could be used to calculate the dendritic to soma ratio for steady diffusional flux under the above-mentioned conditions; it is necessary only to replace the ratio, R_m/R_i, by the ratio, D/P, where D is the intracellular diffusion coefficient (cm^2/sec), and P is the membrane permeability (cm/sec). Thus, for $D = 10^{-5}$ cm^2/sec and $P = 10^{-7}$ cm/sec (34) the average neuron of Table 2 would give a value of about 31 for this diffusional flux ratio. Such diffusional considerations may be relevant to an understanding of factors governing neuronal development and metabolism.

Assessment of Simplifying Assumptions

Isopotentiality of the External Medium. The mathematical theory makes use of the assumption of extracellular isopotentiality. It is obvious that this assumption does not correspond strictly to the situation in nature, and it is desirable to assess the magnitude of discrepancies that might result from this. The gray matter does not provide an infinite conductivity; it is not even a homogeneous conducting medium. The heterogeneity of the interneuronal space is currently under active study (33). This heterogeneity may not produce very much distortion of the extracellular potential field, because the connectivity of the interstitial space must be much more extensive and of finer grain in three dimensions than it appears in a single plane. Thus, it may be hoped that little error results from considering the medium to be homogeneous with an apparent extracellular specific resistance, R_e, that is subject to physical measurement. The gray matter of cat cortex has been found to have an apparent R_e of about

222 Ωcm (16), or approximately four to five times the value of mammalian Ringer (28, p. 470).

For steady radial current flow from inside a spherical soma to a distant external electrode, the potential, V_e, just outside the membrane equals

$$V_e = i\int_b^\infty \frac{R_e}{4\pi r^2}\,dr = \frac{iR_e}{4\pi b}$$

where i is the total radial current and b represents the radius of the sphere. The potential drop, V, across the membrane resistance is simply

$$V = iR_m/(4\pi b^2).$$

Therefore, the ratio of V_e to V is equal to

$$V_e/V = bR_e/R_m.$$

For $b = 30 \times 10^{-4}$ cm, $R_e = 222$ Ωcm and $R_m = 4000$ Ωcm^2, it follows that $V_e/V = 1.5 \times 10^{-4}$; thus V_e differs negligibly from zero, for present purposes.

A similar calculation for a cylindrical membrane, with integration from $r = a$ to $a \times 10^{-3}$, gives the result

$$V_e/V = 6.9aR_e/R_m.$$

For $a = 5 \times 10^{-4}$ cm, $R_e = 222$ Ωcm and $R_m = 4000$ Ωcm^2, it follows that $V_e/V = 1.9 \times 10^{-4}$; here V_e also differs negligibly from zero.[8]

In the early theory of axonal electrotonus, the difficulty of treating the external potential field was recognized by Hermann (19), and was solved for certain boundary conditions, by Weber (30). This mathematical problem has also been studied by Weinberg (31); it involves infinite series of Bessel functions. These complications are usually avoided by limiting consideration either to the case of an axon placed in air or in oil, or to an external volume conductor whose conductivity may be regarded as effectively infinite.

[8] These quantitative considerations were also verified by means of a resistance-capacitance network analog constructed and tested by A. J. McAlister (21). The first analog assumed zero external resistance. Extension to the case of an external medium with finite resistance was accomplished by adding an external resistance network in which the radial increments in resistance were calculated to correspond to cylindrical symmetry in a volume; this type of external resistance network was suggested by K. S. Cole during discussions participated in by W. H. Freygang, Jr., K. Frank, A. J. McAlister, and W. Rall. The experimental tests also revealed a negligible longitudinal gradient of external potential.

Formal solutions of the external field surrounding a spherical neuron with or without cylindrical dendrites have recently been obtained, and will be presented separately.

Isopotentiality of Soma Membrane. Virtual isopotentiality of the soma interior, under resting conditions, has been assumed since the earliest intracellular electrode studies (3). However, the assumption of approximate isopotentiality during the flow of applied or active membrane current is more recent. A theoretical basis for it was provided first for a hypothetical spherical soma;[9] when the electrotonic potential distribution is expanded in terms of Legendre polynomials, it turns out that the higher order terms, which represent the nonuniformity of the electrotonic potential, are smaller than the uniform (zero order) component by a factor whose order of magnitude is $b(R_e + 2R_i)/R_m$, where b is the radius of the sphere. This factor is less than 10^{-3} for mammalian motoneurons. Intuitively, this means simply that the resistance to current flow across the soma membrane is much greater than the resistance to current flow between different points interior (or different points exterior) to the soma membrane. This assumption of soma membrane isopotentiality during current flow was implicit in the calculations of (8), and it has recently become explicit in the discussion of mammalian motoneurons (7, 10, 12, 15, 17, 21, 23–26).

When dendritic current is taken into account, soma isopotentiality does not hold as precisely as for the spherical nerve model. Consider, for example, the unfavorable case of an asymmetric neuron with an intracellular electrode at one end of an elongated soma (or even in a proximal dendrite) and with most of the major dendrites arising at the other end of the soma. If, for example, the soma has major and minor diameters of 90 and 40 μ, and if twenty times more steady current flows across the soma to the dendrites than flows across the soma membrane, then using $R_i = 50$ Ωcm and $R_m = 4000$ Ωcm^2, it can be calculated that the steady potential drop between the two ends of this soma would be about 2 per cent of the steady electrotonic potential of the soma membrane.

Uniform Membrane Resistivity. The value of R_m has been assumed to be the same for the entire soma-dendritic membrane. This is not necessary; the theoretical solutions could be carried out with a different R_m value for the soma and for each cylindrical branch component. In

[9] Preliminary results were presented in 1953 (22), 1955 (23), and 1957 (*Abstracts of National Biophysics Conference,* p. 58); full details have not been published.

particular, since G_N is dominated by the combined dendritic input conductance, the whole neuron value is not very sensitive to postulated changes in the R_m value of just the soma. For example, if we begin with $\rho = 25$, halving the somatic R_m value (12) would reduce R_N by only 4 per cent; reduction of the somatic R_m value by a factor of 10 would reduce R_N by 26 per cent.

The fact that synaptic knobs are distributed in high density over both soma and dendritic membrane surfaces,[10] and the fact that these knobs are packed very close to the membrane surface,[11] suggests that the soma dendritic membrane might have a true resistivity, for unit area, that is lower than the effective value which includes the heterogeneity of the external surface and external volume. Therefore, it should be emphasized that all of the theory and numerical estimates of the present paper are concerned with the effective value of R_m.

Appendix 1. Definition of Symbols

V_e	= extracellular electric potential	G_∞	= input conductance of infinitely extended cylindrical trunk (Eq. [10])
V_i	= intracellular electric potential	R_i	= specific resistance of the internal medium (Ω cm)
V_m	= $V_i - V_e$ = membrane potential	R_m	= resistance across a unit area of membrane (Ω cm^2)
E	= resting membrane potential, and EMF	d	= diameter of cylinder (cm)
V	= $V_m - E$ = electrotonic potential	r_m	= $R_m/\pi d$ = membrane resistance for a unit length of cylinder (Ω cm)
x	= distance along a dendrite, measured from soma	r_i	= $4R_i = \pi d^2$ = internal resistance per unit length of cylinder (Ω cm^{-1})
V_0	= electrotonic potential at $x = 0$	λ	= $[r_m/r_i]^{1/2}$ = characteristic length of cylinder (cm)
i_m	= membrane current density, expressed per unit length of cylinder		= $[(R_m/R_i)\ (d/4)]^{1/2}$
I	= internal (axial) current	d_0	= diameter of trunk
I_0	= internal current at $x = 0$; dendritic input current	λ_0	= characteristic length of trunk
R_D	= V_0/I_0 = dendritic input resistance		
G_D	= I_0/V_0 = dendritic input conductance		

[10] See Rasmussen in Ref. (32).

[11] See, for example, Palay in Ref. (32).

Appendix 1 (*Continued*)

L_0	= length of trunk
B_0	= branching factor (see Eq. [12])
x_1	= value of x at which trunk gives rise to k branches
d_{1k}	= diameter of kth branch arising at $x = x_1$
λ_{1k}	= characteristic length of this kth branch
L_{1k}	= length of this kth branch
B_1	= branching constant at $x = x_1$ (see Eqs. [2] and [16] to [18])
I_1	= internal current at $x = x_1$
V_1	= electrotonic potential at $x = x_1$
x_{2k}	= value of x at end of kth branch arising at $x = x_1$
V_{2k}	= electrotonic potential at $x = x_{2k}$
x_j	= value of x at a general branch point
d_{jk}	= diameter of kth branch arising at $x = x_j$
λ_{jk}	= characteristic length of this kth branch (Eq. [21])
L_{jk}	= length of this kth branch
B_j	= branching constant at $x = x_j$ (see Eq. [19])
$B_{(j+1)k}$	= branching constant at end of kth branch arising at $x = x_j$
d_{j-1}	= diameter of cylinder from which branches arise at $x = x_j$

The following apply to whole neurons:

I_A	= total steady current applied from interior to exterior of neuron
R_N	= V_0/I_A = whole neuron resistance
G_N	= I_A/V_0 = whole neuron conductance
S	= soma surface area
G_S	= S/R_m = some membrane conductance
G_{Dj}	= dendritic input conductance of jth trunk
B_{0j}	= weighting factor of jth trunk at $x = 0$
d_{0j}	= diameter of trunk
$D^{3/2}$	= $\sum_j B_{0j}(d_{0j})^{3/2}$ = combined dendritic tree parameter; compare with combined dendritic trunk parameter, expression [27], and combined dendritic input conductance (Eq. [24])
C	= $(\pi/2)(R_i)^{-1/2}$ (see Eqs. [10] and [24] to [26])
ρ	= ratio of combined dendritic input conductance to soma membrane conductance (Eq. [31]).

References

1. Araki, T., and T. Otani, Response of single motoneurons to direct stimulation in toad's spinal cord. *J. Neurophysiol.* **18**: 472-485, 1955.
2. Balthaser, K., Morphologie der spinalen Tibialis- und Peronaeus-Kerne bei der Katze. *Arch. Psychiatr., Berl.* **188**: 345-378, 1952.
3. Brock, L. G., J. S. Coombs, and J. C. Eccles, The recording of potentials from motoneurones with an intracellular electrode. *J. Physiol., Lond.* **117**: 431-460, 1952.
4. Chu, L. W., A cytological study of anterior horn cells isolated from human spinal cord. *J. Comp. Neur.* **100**: 381-414, 1954.

5. Cole, K. S., and A. L. Hodgkin, Membrane and protoplasm resistance in the squid giant axon. *J. Gen. Physiol.* **22**: 671-687, 1939.
6. Coombs, J. S., D. R. Curtis, and J. C. Eccles, Time courses of motoneuronal responses. *Nature, Lond.* **178**: 1049-1050, 1956.
7. Coombs, J. S., D. R. Curtis, and J. C. Eccles, The electrical constants of the motoneurone membrane. *J. Physiol., Lond.* **145**: 505-528, 1959.
8. Coombs, J. S., J. C. Eccles, and P. Fatt, The electrical properties of the motoneurone membrane. *J. Physiol., Lond.* **130**: 291-325, 1955.
9. Davis, L., Jr., and R. Lorente de Nó, Contribution to the mathematical theory of the electrotonus. *Stud. Rockefeller Inst. M. Res.*, **131**: 442-496, 1947.
10. Eccles, J. C., "The physiology of nerve cells," Baltimore, Johns Hopkins, 1957.
11. Fatt, P., Electrical potentials occurring around a neurone during its antidromic activation. *J. Neurophysiol.* **20**: 27-60, 1957.
12. Fatt, P., Sequence of events in synaptic activation of a motoneurone. *J. Neurophysiol.* **20**: 61-80, 1957.
13. Fisher, R. A., and F. Yates, "Statistical table for biological, agricultural and medical research," New York, Hafner, 1949.
14. Frank, K., and M. G. F. Fuortes, Stimulation of spinal motoneurones with intracellular electrodes. *J. Physiol., Lond.* **134**: 451-470, 1956.
15. Freygang, W. H., Jr., and K. Frank, Extracellular potentials from single spinal motoneurons. *J. Gen. Physiol.* **42**: 749-760, 1959.
16. Freygang, W. H., Jr., and W. M. Landau, Some relations between resistivity and electrical activity in the cerebral cortex of the cat. *J. Cellul. Physiol.* **45**: 377-392, 1955.
17. Fuortes, M. G. F., K. Frank, and M. C. Becker, Steps in the production of motoneuron spikes. *J. Gen. Physiol.* **40**: 735-752, 1957.
18. Haggar, R. A., and M. L. Barr, Quantitative data on the size of synaptic endbulbs in the cat's spinal cord. *J. Comp. Neur.* **93**: 17-35, 1950.
19. Hermann, L., Ueber eine Wirkung galvanischer Ströme auf Muskeln und Nerven. *Pflügers Arch.* **6**: 312-360, 1872 (ref. pp. 336-343).
20. Hodgkin, A. L., and W. A. H. Rushton, The electrical constants of a crustacean nerve fibre. *Proc. R. Soc., Ser. B., Biol. Sc., Lond.* **133**: 444-479, 1946.
21. McAlister, A. J., Analog study of a single neuron in a volume conductor. *Naval M. Res. Inst., Research Reports* **16**: 1011-1022, 1958.
22. Rall, W., Electrotonic theory for a spherical neurone. *Proc. Univ. Otago M. School* **31**: 14-15, 1953.
23. Rall, W., A statistical theory of monosynaptic input-output relations. *J. Cellul. Physiol.* **46**: 373-411, 1955 (ref. p. 403).
24. Rall, W., Membrane time constant of motoneurons. *Science* **126**: 454, 1957.
25. Rall, W., Mathematical solutions for passive electrotonic spread between a neuron soma and its dendrites. *Fed. Proc., Balt.* **17**: 127, 1958.
26. Rall, W., Membrane potential transients and membrane time constant of motoneurons. *Exp. Neur.* **2**: 1960 (in press).
27. Ramón y Cajal, S., "Histologie du système nerveux de l'homme et des vertébrés," vol. 1, Paris, Maloine, 1909.

28. Tasaki, I., E. H. Polley, and F. Orrego, Action potentials from individual elements in cat geniculate and striate cortex. *J. Neurophysiol.* **17**: 454-474, 1954.
29. Van Harreveld, A., Changes in volume of cortical neuronal elements during asphyxiation. *Am. J. Physiol.* **191**: 233-242, 1957.
30. Weber, H., Ueber die stätionaren Strömungen der Elektricität in Cylindern. *Borchardt's J. Math.* **76**: 1-20, 1873.
31. Weinberg, A. M., Weber's theory of the kernleiter. *Bull. Math. Biophysics* **3**: 39-55, 1941.
32. Windle, W. F. (ed.), "New research techniques of neuroanatomy," Springfield, Illinois, Thomas, 1957.
33. Windle, W. F. (ed.), "Biology of neuroglia," Springfield, Illinois, Thomas, 1958.
34. Zwolinski, B. J., H. Eyring, and C. E. Reese, Diffusion and membrane permeability. *J. Phys. Colloid. Chem.* **53**: 1426-1453, 1949.

The Theoretical Foundation of Dendritic Function

The Collected Papers of Wilfrid Rall with Commentaries

Edited by: Idan Segev, John Rinzel, Gordon M. Shepherd

Citation:

The Theoretical Foundation of Dendritic Function: The Collected Papers of Wilfrid Rall with Commentaries
Edited by: Idan Segev, John Rinzel, Gordon M. Shepherd
DOI: 10.7551/mitpress/6743.001.0001
ISBN (electronic): 9780262283373
Publisher: The MIT Press
Published: 2003

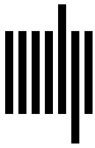

The MIT Press

This book was published with the assistance of the Office of Naval Research and the National Institute of Diabetes and Digestive and Kidney Diseases, National Institutes of Health.

This book was printed and bound in the United States of America.

Library of Congress Cataloging-in-Publication Data

Rall, Wilfrid.
The theoretical foundation of dendritic function : selected papers
of Wilfrid Rall with commentaries / edited by Idan Segev, John Rinzel, and
Gordon M. Shepherd.
p. cm. — (Computational neuroscience)
"A Bradford book."
Includes bibliographical references.
ISBN 0-262-19356-6
1. Dendrites—Mathematical models. I. Segev, Idan. II. Rinzel, John. III. Shepherd,
Gordon M., 1933– IV. Title. V. Series.
QP361.R33 1995
612.8—dc20 94-13538
CIP